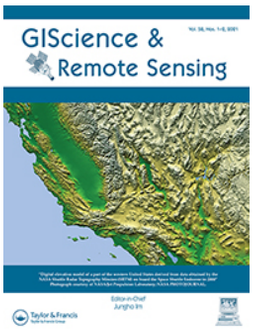

GIScience & Remote Sensing

ISSN: (Print) (Online) Journal homepage: www.tandfonline.com/journals/tgrs20

Assessment of intersection conflicts between riders and pedestrians using a GIS-based framework and portable LiDAR

Keila González-Gómez, Serafín López-Cuervo Medina & María Castro

To cite this article: Keila González-Gómez, Serafín López-Cuervo Medina & María Castro (2021) Assessment of intersection conflicts between riders and pedestrians using a GIS-based framework and portable LiDAR, GIScience & Remote Sensing, 58:4, 587-602, DOI: 10.1080/15481603.2021.1920199

To link to this article: https://doi.org/10.1080/15481603.2021.1920199

GISCIENCE & REMOTE SENSING
2021, VOL. 58, NO. 4, 587–602
https://doi.org/10.1080/15481603.2021.1920199

Taylor & Francis
Taylor & Francis Group

Assessment of intersection conflicts between riders and pedestrians using a GIS-based framework and portable LiDAR

Keila González-Gómez [a], Serafín López-Cuervo Medina [b] and María Castro [a]

[a]Departamento de Ingeniería del Transporte, Territorio y Urbanismo, Universidad Politécnica de Madrid, Madrid, Spain; [b]Departamento de Ingeniería Topográfica y Cartográfica, Universidad Politécnica de Madrid, Madrid, Spain

ABSTRACT

Adequate sight distances are crucial parameters ruling the design of roads and riding facilities. LiDAR-retrieved data have proved to serve many transportation applications by creating updated and accurate representations of the road environment. As a result, many sight distance evaluation methodologies use LiDAR delivered point clouds to carry out visibility analyses. However, current approaches are mainly focused on motorized users along highways and streets, and most of those methodologies are carried out directly on the point cloud, which does not allow the evaluation or relocation of visual obstructions. This study presents a visibility-based procedure intended to assess the circulation of pedestrians and riders at urban intersections. For this purpose, first, the required sight distances of all users along the intersection are obtained. Second, the conflicts between vulnerable road users are evaluated, considering the type of control present at the intersection. The available sight distances are then obtained using a GIS-based method that employs 3D road models derived from the LiDAR retrieved data. Finally, after a comparison between the required and the available visibility, an evaluation determines which user sees a larger percentage of the intersection. This approach facilitates evaluating the impact that vegetation, traffic, and/or furniture elements could have on visibility and serve as an urban design aid tool. Results show that the proposed method offers valuable insights into the distributions of visibility among intersecting users and into the quantifications of the effect of specific adjacent traffic. Moreover, this procedure stands as a useful and flexible approach that allows the evaluation of both cyclists and e-scooter riders in different road facilities and positionings.

ARTICLE HISTORY
Received 18 January 2021
Accepted 17 April 2021

KEYWORDS
Portable LiDAR; GIS; visibility analyses; urban intersections; road safety

1. Introduction

Sight distance is the continuous length of a roadway that is visible to drivers and other road users. Specific distances are required to carry out basic driving maneuvers such as stopping, passing, or crossing; consequently, most road design guidelines state minimum sight distance values for these maneuvers (AASHTO, 2018; AUSTROADS 2016; Ministerio de Fomento 2016). To a similar extent, bicycle facilities and sidewalks ought to be provisioned with specific distances and clear lines of sight to allow their users to spot other road users, be aware of the presence of physical elements, and minimize the risk of conflicts.

During the design stage, these required sight distances impact the final dimensions of the elements that compose highways, streets, and bikeways and need to be periodically assessed during operation. These assessments compare the required sight distances with the available sight distances, sometimes by means of troublesome field measurements. Due to its impact on the efficient and safe performance of roads, the estimation of available sight distances on existing roads has been a topic explored by several researchers. Some of them have proposed analytical and graphical methods intended to highlight the shortcomings of sight distance evaluations carried out two-dimensionally (Hassan, Easa, and El Halim 1996; Sanchez 1995). However, these methodologies are not designed for assessments that consider the current state of existing roads, where obstructions caused by vegetation growth or manmade structures could arise. Because estimations that evaluate the state of existing roads require detailed and updated digital representations of the road environment, many transportation applications employ photogrammetry or LiDAR-based mobile mapping systems (MMS) for road modeling purposes (Gargoum and El Basyouny 2019). In this regard, many visibility

CONTACT María Castro maria.castro@upm.es

analyses have taken advantage of the up-to-date road models provided by LiDAR-based systems (Castro et al. 2016; González-Jorge et al. 2016; Khattak and Shamayleh 2005; Zhao et al. 2020). These scanning systems allow quantifying the impact of common obstructions, such as street furniture or road assets, and they also enable the evaluation of their relocation or re-dimensioning. Nevertheless, LiDAR-based estimations that are carried out in geographic information systems (GIS) environments and make use of traditional digital surface models (DSM) are unable to portray the road environment in a fully 3D fashion. This is because widespread DSM formats are unable to render more than one height per x, y position. Therefore, analyses carried out using these formats are 2.5 D. Highly dense point clouds are able to portray realistic 3D representations of the road environment, for that reason, current LiDAR-based methodologies detect obstructions directly on them, without the need for modeling processes. Olsen et al. (2016) presented a procedure to evaluate visibility from different perspectives using voxelized point clouds. Ma et al. (2019) also showed an innovative point cloud-based methodology employing neural networks to improve its efficiency. These methodologies were tested by evaluating the sight distances of motorized users so as to be compared to their stopping sight distances and intersection sight distances.

At-grade intersections constitute one of the most complicated roadway elements due to the wide variety of movements they host (AASHTO, 2018). However, fewer contributions have been explicitly intended at assessing their visibility, and even fewer have been made considering vulnerable road users (e.g., pedestrians or cyclists) as main observers. In terms of safety, research carried out by the Federal Highway Administration (FHWA) evidenced that bicycle-to-bicycle injuries are high in number but less reported (Stutts and Hunter 1999). Moreover, their likelihood is augmenting as more riders are welcomed on roads and streets (Cai, Abdel-Aty, and Castro 2020). A report showing a compilation of road crashes that occurred in the United States in 2014 evidenced that the second factor involved in the majority of accidents comprising pedestrians or cyclists was lack of visibility (National Highway Traffic Safety Administration 2017). Most authors have evaluated the visibility available at road intersections by means of their sight triangle. These triangles are definite intersection areas that should be free of obstructions (Harwood et al. 1996). Khattak, Hallmark, and Souleyrette (2003) evaluated the required sight triangles at road intersections launching equally spaced lines-of-sight on LiDAR retrieved DSM. Similarly, Tsai, Yang, and Wu (2011) quantified the obstructions present at urban intersections, comparing the viewshed of the observers with their required sight triangle. These evaluations were carried out in 2.5 D. Other authors presented point cloud-based 3D methodologies from LiDAR-retrieved data, where the sight distances of motorized users were obtained by means of their viewshed (Jung et al. 2018). However, all these methodologies were implemented on the roadway and did not include sidewalk or bikeway evaluations. In that regard, creating detailed 3D models of segregated cycling and walking facilities is less straightforward than that of roadways. Vehicle-fixed MMS are too wide to fit their narrow cross-sections. When mapped from the roadway, separating elements such as dense bushes or road furniture elements are likely to block laser beams or photos. Portable MMS appears as a solution to these constraints; however, their use is less common than airborne, terrestrial, or mobile. Nonetheless, the advantages related to their portability (Karam et al. 2019), accuracy (López-Cuervo Medina et al. 2019), and deployment are well documented. Regarding the use of portable MMS to estimate sight distances, Bassani, Grasso, and Piras (2015) employed an image-based MMS mounted on a bike to generate DSMs of bikeways and evaluate the sight distances needed for stopping.

Most existing methodologies for visibility evaluation are limited to the consideration of a single observer, usually a motorized user. They also did not include the evaluation of conflicts among vulnerable users, which compose a high percentage of traffic conflicts taking place in urban settings (Stutts and Hunter 1999). Furthermore, most of them do not include functionalities intended to facilitate the repositioning or dimensioning of the encountered obstructions. These simply identify them as obstructions and categorize them for removal. To address this issue, the main goal of this paper is to propose a procedure to evaluate the visibility among riders and pedestrians at intersections, including segregated paths and sidepath junctions. This study evaluates the visibility of both observer and target and their successive positionings along the junction

toward their conflict point. In addition, fully 3D evaluations are carried out by means of two models: a digital terrain model (DTM) portraying the road geometry and another one describing aboveground elements. This is done with the intention of creating scenarios aimed at evaluating the positioning and/or dimensions of indispensable urban furniture elements or road assets. Moreover, the separate consideration of aboveground enables the introduction of 3D objects, allowing the assessment of the impact that different traffic set-ups have on visibility. Secondary goals are to test the usefulness and suitability of point clouds delivered by portable LiDAR systems to carry out sight distance assessments. Requirements such as the area covered, resolution, productivity, and accuracy were evaluated.

This paper is structured as follows: The next section contains a detailed description of the proposed procedure, including a description of the case study, data acquisition, and processing. Subsequently, results are presented and discussed, and finally, the main conclusions are outlined.

2. Methodology

2.1 Procedure

This study proposes a procedure to evaluate and quantify visibility among users of intersections. This includes evaluations on the roadway, sidewalks, and off-road facilities. Intersection users to be evaluated are riders (cyclists or e-scooter users) and pedestrians. The procedure is divided into two phases. The first one evaluates conflicting movements between riders, and the second one handles conflicts between riders and pedestrians. Figure 1 illustrates the first phase, where RSD stands for required sight distances, SSD for stopping sight distances, ISD for intersection sight distances, and ASD stands for available sight distances.

The first step, within the gray rectangle, can be carried out by means of polylines describing the geometry of the roadway, bikeway, and/or sidewalks in addition to their design and operation properties. Required sight distances can be obtained using GIS or road design software. Sight distance estimations and intervisibility calculations are carried out using a geoprocessing model that requires 3D trajectories, road design parameters, traffic parameters, and 3D representations of the roadway, sidewalks, and off-road facilities (if present).

The second phase comprises the evaluation of conflicts between riders and pedestrians by launching lines-of-sight from the bikeway aimed at the sidewalk with particular interest in their convergences.

The following paragraphs describe the main steps of phase 1, presented in Figure 1. These steps are as follows:

- Step 1: Determine the required sight distances: stopping sight distances and intersection sight distances.
- Step 2: Estimate available sight distances for stopping maneuvers.
- Step 3: Compare the available sight distances to stopping sight distances.
- Step 4: Verify if conflicts between riders are handled by the type of intersection control.
- Step 5: Estimate the available sight distances needed on at-grade intersections.
- Step 6: Compare the available sight distances to intersection sight distances.

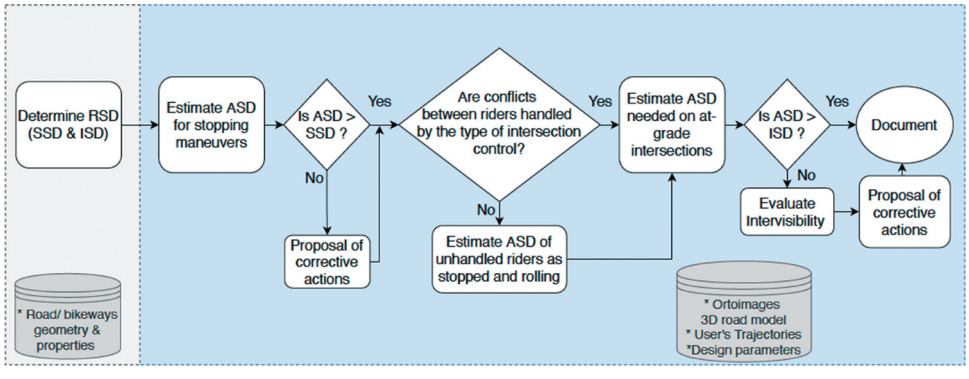

Figure 1. Flowchart describing the first part of the proposed procedure.

2.1.1 Step 1: determine required sight distances: stopping and intersection

The required sight distances with more impact on the final disposition of the design elements that constitute cycling facilities are stopping sight distances and intersection sight distances (AASHTO 2012; AUSTROADS 2017a). Stopping sight distances are required along the whole traveled way, and intersection sight distances determine the size of the intersection area that should be unobstructed.

The main factors involved in the stopping maneuver are initial speed, perception and reaction time, the grade, the vehicle's breaking ability as well as the coefficient of friction between the pavement and the tire. These parameters can be specific to definite road segments and could change from one road station to another. Moreover, they are used to determine the minimum stopping sight distances, as shown in equation (1) (AASHTO 2012).

$$S = \frac{v^2}{254(f \pm G)} + \frac{v}{1.4} \quad (1)$$

Where:

S = minimum stopping sight distance, m

v = initial speed of the rider, km/h

f = coefficient of friction between the road surface and the tire

G = slope, m/m

When it comes to intersections, sight distances formulations vary depending on the type of junction under study, the type of control established at the intersection, and other factors. Several road design guidelines detail how these factors determine the value of intersection sight distances (AASHTO, 2018; AUSTROADS 2017b; Ministerio de Fomento 2016, 2012). This value defines the size of the sight triangles (the intersection area that should be clear of obstructions). Figure 2 shows the general configuration of required sight triangles. These apply for riders on the roadway and on bikeways.

Figure 2 shows the conflict point, which is where conflicting trajectories meet each other. The decision point, where road users without the right of way decide if they are able to cross or not. The target point is located in a conflicting trajectory at a distance from the conflict point that would allow approaching drivers or riders to stop safely. The sight line is the one that both users require to recognize each other, and the clear sight triangle, as previously defined, is the intersection area that should be free of obstructions. Once the dimensions of these legs are obtained, a sight plane is conceived by adding the eye heights of observers and targets. Elements that are above or below this plane are not necessarily visual obstacles (Harwood et al. 1996).

The parameters commonly included in intersection sight distance formulae, for both legged and circular intersections, are the speed of the road user considered as observer, and its perception and reaction time. This is exemplified in equation (2) (AASHTO 2012):

$$ISD = 0.278vt_a \quad (2)$$

Where:

ISD = intersection sight distance, m

v = initial speed, km/h

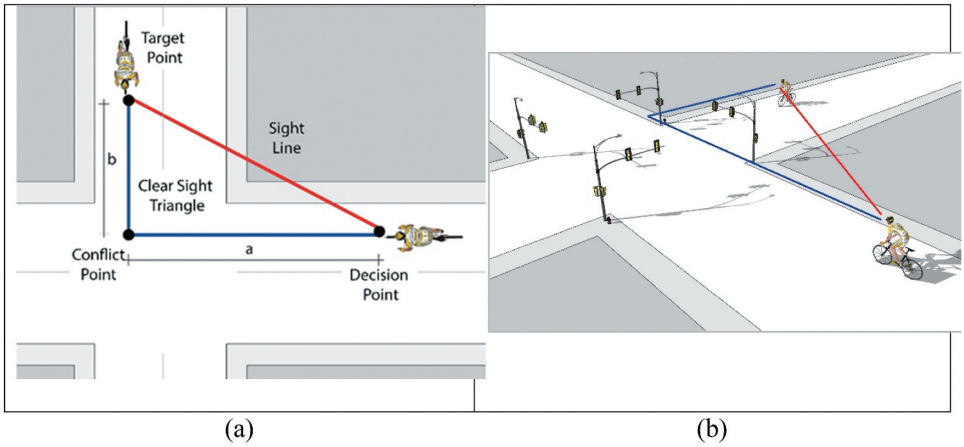

Figure 2. Elements that constitute intersection sight triangles in a top view: decision, conflict and target points, and sight line (a); perspective view (b).

t_a = the travel time to reach the road, measured from the decision point and considering a path user that is not going to stop, s

2.1.2 Step 2: estimate available sight distances for stopping maneuvers

Procedures that estimate available sight distances for stopping maneuvers are commonly done launching sightlines toward an object placed on the observer's path. The presented procedure launches these sightlines by means of a geoprocessing model based on GIS tools. The model takes as input parameters a DTM describing the road geometry and roadside terrain, a multipatch file describing the aboveground elements, and the trajectory of the observer with its eye-height. First, trajectories are turned into successive and equally distanced points: D1 = {D1, D2, D3 … Dn-1, Dn $|n \in N+\}$. Since both the observer and target are located on the same trajectory, this evaluation only requires one trajectory describing their path. The position of the trajectory along the roadway as well as the heights of observer and object varies from one guideline to another. Guidelines from the American Association of Highway and Transportation Officials (AASHTO) stipulate that measurements can be performed along the centerline or traveled-way edge. In the same way, it stipulates that, for drivers, the eye-height is 1.08 m and for cyclists 1.4 m. These are absolute values regardless of age and gender. The object's height is 0.6 m for motorized users, and for cyclists or riders, the object could be considered at a 0 m height (AASHTO, 2018; AASHTO 2012).

In order to depict the road environment, a LiDAR-derived DTM is employed in combination with 3D files. These 3D files, also obtained from the point cloud, represent aboveground elements such as vegetation and manmade structures. These features could also include elements that are not present at the time of data acquisition and/or those whose impact on visibility is to be evaluated. As many urban analyses have taken advantage of extracting city elements from LiDAR retrieved point clouds (Cao et al. 2020), it is more common to count with 3D files that represent urban assets, buildings and more. In addition, these 3D files could also be shaped utilizing 3D modeling software such as SketchUp (Trimble 2018). Moreover, trusted widespread open-source city models such as CityGML or COLLADA files could also be used. These 3D files could be inserted into the multipatch file where multiple scenarios could be evaluated. With these inputs, the model is capable of verifying which elements, terrain or aboveground, obstruct the visibility. As a result, the model delivers a depiction of the sightlines, whether obstructed or not and a point file with the exact location of the obstruction.

2.1.3 Step 3: compare the available sight distances to stopping sight distances

After the available sight distance is estimated, it has to be compared to the stopping sight distances. Due to the fact that stopping sight distances have to be provisioned along the whole bikeway, the length of the segment under evaluation depends on the available data, processing capacities or a possible selection of segments with proven deficiencies. As stopping sight distance values vary with the speed of the segment and the grade, these change along the trajectory the required value will vary accordingly. This procedure eases the comparison by providing a list of the unobstructed sight distances of every station and their chart. The comparison is performed station-wise and locations where the availability is less than the required individually inspected.

2.1.4 Step 4: verify if conflicts between riders handled by the type of intersection control

The revised guidelines and standards explain the importance of verifying if conflicts between riders and motorized traffic (cars, trucks, etc.) are appropriately accounted for (AASHTO 2012; AUSTROADS 2017a; Ayuntamiento de Madrid 2008; Ministerio de Fomento 2016, 2012). In addition to that, it is also important to evaluate if users of off-road cycling facilities are able to identify each other. It is known that the establishment of the type of control present at road intersections obeys different traffic and geometric design considerations (some related to sight distances). If the type of control established does not solve conflicts among riders, this methodology proposes their evaluation in two distinct scenarios: stopped and rolling.

2.1.5 Estimation of available sight distances of unhandled riders as stopped and rolling

This differentiated evaluation is based on the fact that the speed and performance of riders are dependent on whether they arrive at a stop or yield a controlled

junction or at a green traffic light versus a red one (Romanillos and Gutiérrez 2019). In the first scenario (stop or yield controlled junction), users are considered to be stopped or about to stop. The second one (green traffic light) considers them to be moving with the intention to cross and interact with other users. Consequently, for each case, trajectories, scanning behavior and targets are different. Stopped users are considered to be at or near the crossing, whereas rolling ones are depicted at distances equal to the value of their intersection sight distance measured from the intersection's edge. These assessments are described as follows:

- Stopped ones are those bicyclists or riders arriving at a red light or yield or stop sign at the intersection. This state includes those already at the crossing point waiting for their time to cross, as well as those that could be on the move but eventually coming to a full stop. Their evaluation areas are similar to that of departure sight triangles. These riders are supposed to be provisioned with sufficient sight distances so as to see sections ahead of their trajectory as well as conflictive ones. As these users are located at the edge or near the crossing point (Figure 3 (a)), a large section of their required sight triangle covers the roadway, and there, the main obstacles are caused by present traffic. For that, this procedure proposes an evaluation of the impact of different levels of traffic volumes on their available sight distances.
- Rolling riders are those bicyclists or riders arriving at a green light or at an uncontrolled intersection. These cyclists and riders are the ones approaching the intersection with the right of way and proceeding to turn or cross it without necessarily coming to a full stop. Analogous to this, uncontrolled intersections function under the assumption that drivers approaching do not need to stop unless it is essential. Hence, both legs of their clear sight triangle depend on the speed of approaching users, as in Figure 3 (b). Being this the case when two conflicting riders describe potentially conflicting trajectories while simultaneously having the right of way. The approach sight triangle illustrated in Figure 3 (b) is assessed for these users.

2.1.6 Step 5: estimate the sight distances needed on at-grade intersections

The previous evaluation estimates the available sight distance of unhandled riders. The rest of trajectories should be also assessed.

In addition to the use and evaluation of sightlines, the visibility of road intersections is usually estimated using viewsheds. In this study, the available sight distances are obtained assessing sightlines that are within the required sight plane. These sightlines are launched toward users located at conflicting trajectories. The model and input data used is the same as the one described in step no. 2. The difference on this assessment is that this procedure requires two trajectories, one for the observer D1 = {D1, D2, D3 . . . Dn-1, Dn $|n \in N+\}$ and another one for the conflicting user

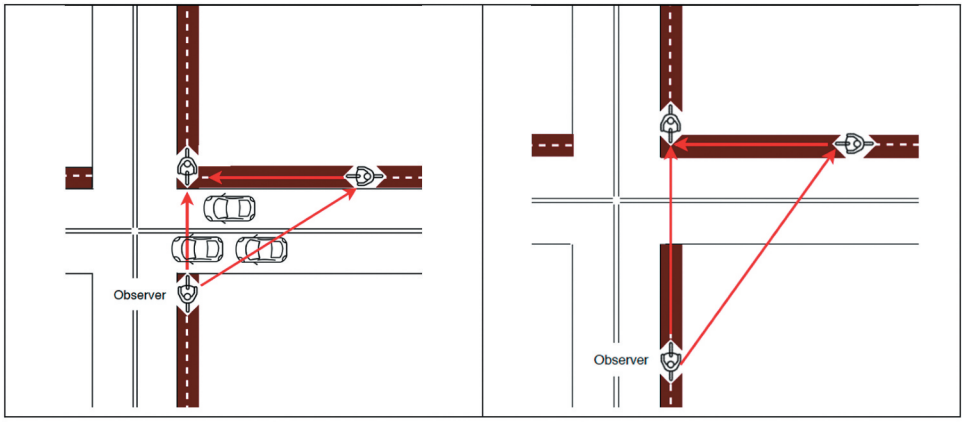

Figure 3. Intersection sight triangles for the evaluations proposed: (a) Stopped observer with a departure sight triangle; (b) Rolling observer in an approaching sight triangle.

T1 = {T1, T2, T3 . . . Tn-1, Tn $|n \in N+\}$, in separate files. The exact lane positioning of both observer and observed varies from one guideline to another. Their eye height depends on which road user is considered an observer and which is consider as conflicting. The eye height of cyclists is 1.4 m as stipulated in the guidelines (AASHTO 2012); e-scooter riders are considered to have an eye-height of 1.8 m, and pedestrians 1.7 m. After observers and targets are correctly placed in the model, the required sight plane is determined using the intersection sight distance values. Next, the lines-of-sights are launched and evaluated.

2.1.7 Step 6: compare the available sight distance to the intersection sight distance

This comparison checks for elements blocking the sight triangle. Once the required sight plane is placed in the model, the sightlines within this triangle are examined and the percentage of them that are blocked would represent its visibility. If this comparison highlights that a larger percentage of the sight triangle is not visible, the intervisibility of both road users involved is estimated and compared.

2.1.8 Evaluate intervisibility

This evaluation launches sightlines twice, from observer to target and back from target to observer. Results from this evaluation are the lines-of-sights between observer one aiming at observer two, the line-of-sight between observer two aiming at observer one, and files with the exact location of the elements that caused the obstructions between them. The files containing these sightlines specify the visibility between the considered observer and target with values 0 and 1. Value 1 means the line that connects them is visible (non-obstructed). If the considered target is not visible, not only is the value 0 but also the sightline is divided into two parts, one that goes from the observer to the obstruction and the other linking the obstruction to the targeted observer. Those segmented sightlines are normalized in values ranging from 0 to 1 depending on how much of the total trajectory toward their respective target they are able to see. This is later used to determine which leg of the triangle has more visibility toward the other. This evaluation could be useful to prioritize interventions between sides of an intersection and to understand the behavior of intersecting bikeway users. Once all the sightlines from both observers are uniform in terms of 0 to 1, it is possible to carry out statistic tests to determine differences between the two samples. The first sample includes the visibility values ranging from 0 to 1 from the sightlines connecting observer to a target, and the second sample those from targets (observers 2) to observers. This difference is obtained by means of the least significant difference (LSD) test (equation (3)). This test helps to identify if the means of two populations are statistically different (Williams and Abdi 2010):

$$LSD = t_{\left[\frac{0.05}{2},(a-1)(b-1)\right]}\sqrt{\frac{2*MS\ error}{b}} \quad (3)$$

Where:

a = the number of directions considered

b = the number of runs

MS = the squared mean error

Once the significance of the differences in visibility between riders is obtained if the test determines that they are indeed significant, the percentage of the sight triangle that they are able to see is estimated. This is done by calculating the percentage of visible sightlines within the required sight triangle for each user.

2.1.8 Phase 2

Phase two evaluates and quantifies conflicts between riders and pedestrians. AASHTO guidelines establish fixed dimensions triangles that would allow pedestrians to spot riders approaching the sidewalk from a sidepath (Figure 4).

These evaluations are recommended in midblock intersections, where pedestrians could not be expecting cyclists. Nonetheless, many sidepath crossings located within the functional area of roadway intersections could contain sign and post clutter that might block the lines-of-sight needed by these users.

2.2 Case study description

Two intersecting bikeways located in Madrid, Spain, were analyzed. The first one constitutes a segregated sidepath located on the northbound side of Av. Complutense. The second one is a bikeway on the right-side sidewalk of Prof. Novais Street. Figure 5(a) shows the geometry of the intersecting bikeways painted in dark red, and the sidewalks in light gray and blue points show the location of conflict points. These bikeways have average widths of 3 m, and two

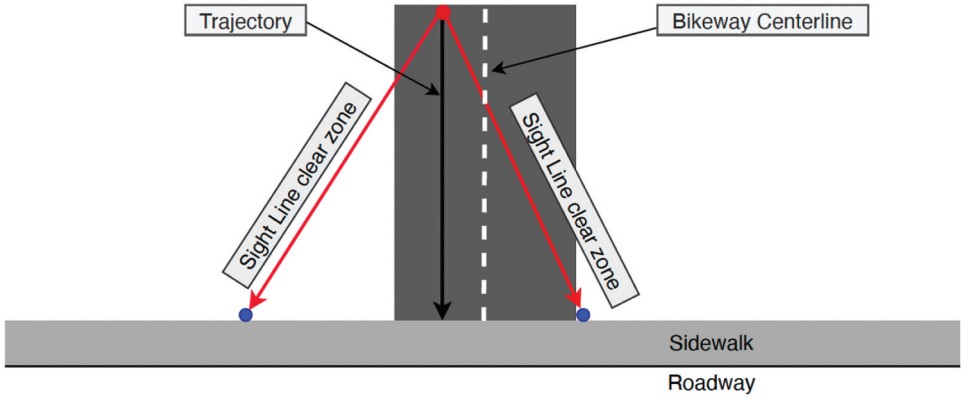

Figure 4. Clear sight zones required to avoid pedestrian-rider conflicts.

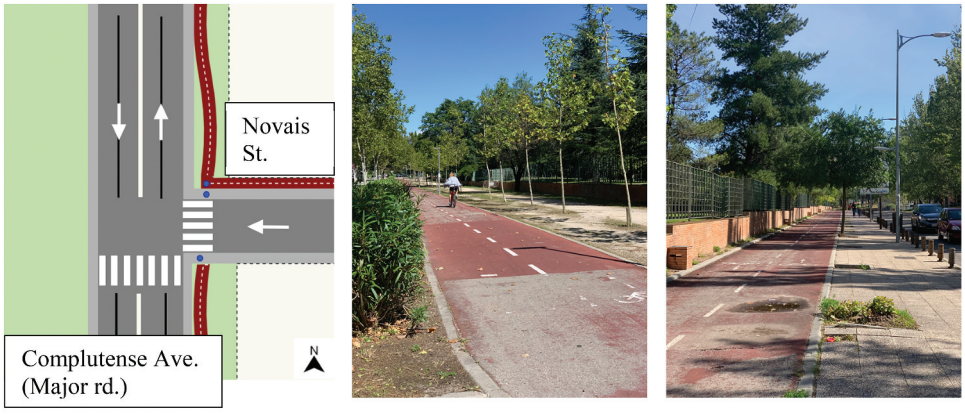

Figure 5. Case study description: (a) intersection geometry, (b) sidepath along Complutense Ave., (c) cycle track adjacent to Novais St. sidewalk.

lanes, one for each direction of travel, as photographed in Figures 5(b) and 5(c). The lanes are separated by a 10-cm-wide intermittent white stripe. The sidepath adjacent to Complutense Ave. is segregated from the sidewalk by a landscaped strip with shrubs, and benches. Likewise, the sidewalk is separated from the roadway by a landscaped strip and bollards. The second bikeway, a cycle track next to José Antonio Novais' street is separated from the sidewalk by a succession of equally spaced plants. Some of these plants are medium-height trees, but the majority are small shrubs.

Due to the fact that these paths are located inside the university district, the volumes of pedestrians tend to be heavy, and it is usual to find pedestrians walking inside the cycling area. Furthermore, these surroundings are populated with app-based dockless e-scooters and e-bikes systems from different companies along with public transportation options (bus and metro). These two bikeways intersect at a signalized T-junction between Complutense Ave. and José Antonio Novais St. These roads have posted speed limits of 30 km/h and 20 km/h, respectively. Complutense Ave. has two lanes for each direction, which are separated by a ~2.8 m median. José Novais St. is a one-way road with two lanes. The average width of the lanes of both streets is 3.4 m.

2.3 Data acquisition and processing

The procedure described requires highly accurate 3D models of the road, roadside elements, and cycling facilities. These could come from distinct sources. Data utilized in this case study were collected employing the MMS Leica Pegasus Backpack (Leica Geosystems 2020) (Figure 6). The system is a wearable solution aimed at capturing calibrated imagery and point cloud data. Its main components are a

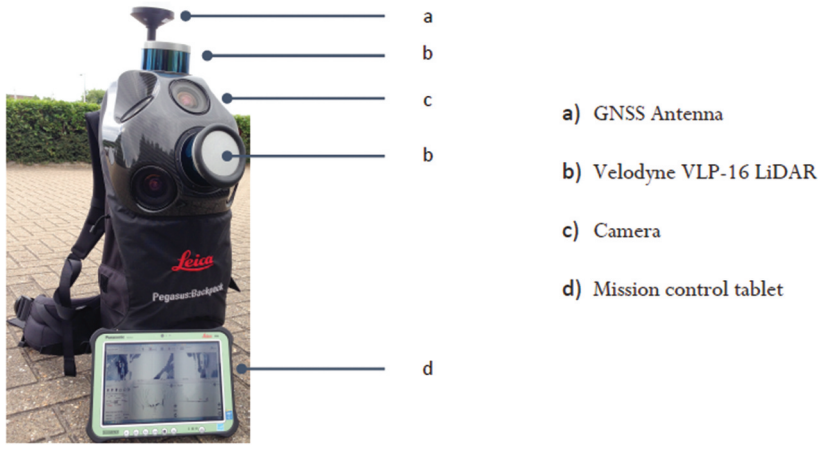

Figure 6. Portable LiDAR system Leica Pegasus Backpack.

navigation system (with a global navigation satellite system (GNSS) receiver along with an Inertial Navigation System), five cameras, a control unit, and a dual laser scanner. The camera coverage is 360° x 200°. The scanner is a Dual Velodyne VLP 16. This sensor has 16 channels and a range accuracy of up to ±3 cm. Its vertical angular resolution is 2.0°, and the horizontal one (Azimuth) ranges from 0.1° to 0.4°. The horizontal field of view of the scanner is 360° although the whole system can obtain 270°. The vertical field of view is +15° to −15° (30°). This scanner is capable of obtaining 600,000 points per second in its dual-return mode at a rotation rate of 10 Hz. The scanner has a range of 100 m, but the backpack system specifies a usable range of 50 m. This system adds to its simultaneous localization and mapping (SLAM) algorithms the GNSS receiver Novatel Propak 6. Its relative accuracy is 2 cm for outdoor environments, and its absolute accuracy is 5 cm (Leica Geosystems 2020). The system was calibrated by the vendor, and the specifications of the desired deliverables were discussed in meetings prior to the survey date, including the election of the network that would be used for GNSS postprocessing.

The human operator carrying the system was 1.91 m high, his speed as well as the satellite coverage were closely followed up using the control tablet. The survey was carried out walking along the bikeways and sidewalks at a relatively constant speed, avoiding sudden, abrupt, or quick movement. This intersection was mapped in about 30 minutes. Therefore, the system's battery life of 3 hours was not a problem. The coverage of each sidewalk side allowed the acquisition of elements that were blocked by stopped traffic and pedestrians. The georeferencing and registration of the data delivered by the system were carried out by the vendors with the software Inertial explorer and AutoP. GNSS observations were post-processed utilizing data from the HxGN SmartNet Network. The point clouds of the whole survey were divided into files of 20,000,000 points in the LAS format. The denoising, classification, and filtering were performed in-house using the software MDTopX (Digi21 2018). This software has functionalities dedicated to processing LiDAR data captured with MMS. First, the ground classification was carried out using a functionality that uses the trajectory of the mapping system, the orientation of the scanners and neighboring properties. After that, the elements that belonged to edifications, trees, road assets, and others were filtered. Points classified as ground were used to generate the DTM, in the vector-based triangulated irregular network (TIN) format, representing the geometry of the bikeways, roadway and sidewalks. Elements classified as aboveground features were used to generate the multipatch object depicting potential obstructions.

2.4 Data modeling

The delivered data from the portable LiDAR provided sufficient accuracy and resolution to produce models that depicted a correct representation of the case study junction. The point resolution along the whole area was fine (more than 100 points per m^2). The resulting point cloud comprised 220 million points, from which the DTM and 3D multipatch files were

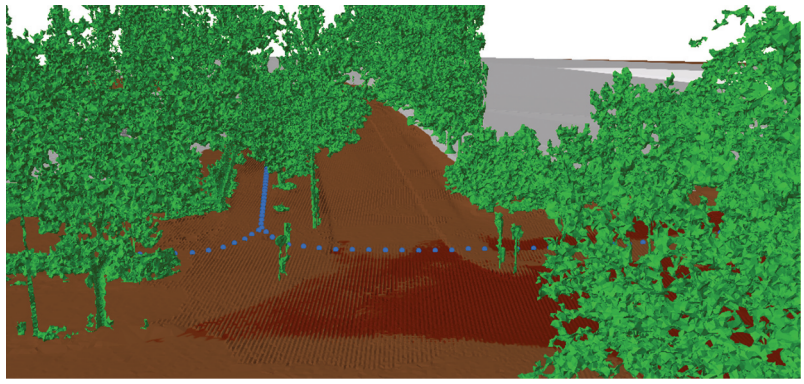

Figure 7. GIS elements modeling the intersection: multipatch objects (green) on top of the terrain model (brown and gray); trajectories are depicted by blue dots.

generated. The average point cloud spacing was 0.02 m with horizontal and vertical accuracy of less than 10 cm. The above-ground elements are represented by polyhedral entities, with a 20 cm separation between edges. This separation was selected considering both the efficiency of the model and the accuracy of the resulting point cloud.

As mentioned above, the geometry of the road and terrain were modeled by means of a DTM, with a 0.2 m grid size. This grid size followed performance considerations. All these elements, as well as the trajectories, are illustrated in Figure 7.

Figure 7 depicts the virtual representation of a portion of the case study. The blue dots represent the discretized trajectory, green entities (3D multipatch files) emulate the vegetation and other above-ground elements, and the DTM is portrayed in brownish and gray shades. These colors were assigned following aesthetic considerations.

3. Results and discussions

The described procedure in section 2 was applied to the case study junction. The main results are presented herein.

3.1 Available vs stopping sight distances

The minimum stopping sight distances for cyclists and e-scooter riders were obtained with equation (1). Its value for riders in the minor road was 24.12 m and for riders along the major road was 43.57 m. Additionally, these values considered a perception and reaction time of 2.5 seconds as stipulated in the guidelines (AASHTO 2012).

The evaluation of the distances required to perform a stopping maneuver was carried out using an eye height of the observer of 1.4 m for cyclists and 1.8 m for e-scooter riders. The height of the object was 0.20 m, a higher value than the one specified in the guidelines. This was done with the intention of evaluating the impact of objects hovering over/around the bikeway and not exactly on it.

The stopping and available sight distances were obtained for all the allowed movements within the intersection. The individual length of the trajectories was 197 m in average. Only two trajectories lacked stopping sight distances. These were northbound and southbound riders along the major road. An inspection of the model revealed that the visual obstructions were mainly caused by the segregating landscaping strip. The same medium height shrubs caused obstructions to southbound riders. In order to quantify the impact of these medium height shrubs, a new scenario (called scenario 2) was created. In this scenario, the real vegetation was removed from the model and replaced by 3D objects depicting generic shrubs (Figure 8).

These objects were obtained and later modified from the software and warehouse SketchUp (Trimble 2018). Their main difference from the real shrubs was their uniformity, and lack of lose branches that could occupy the bikeway. After these objects replaced the real shrubs, the analysis was a rerun. Figure 9 shows these results. It shows a comparison between available (blue and green lines) and required sight distances (orange line) for the two scenarios. The blue

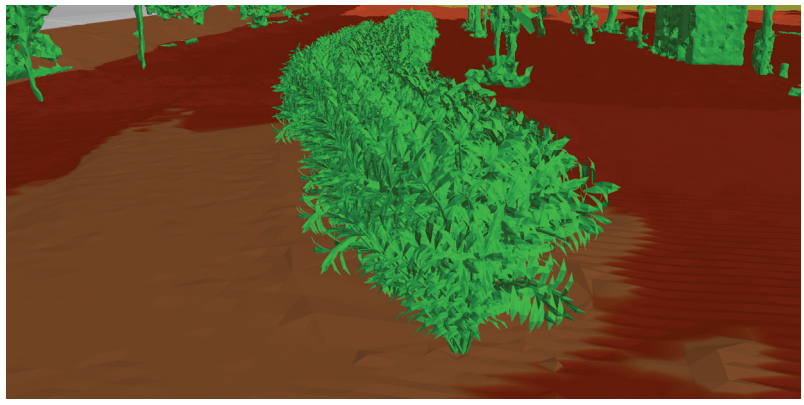

Figure 8. 3D object used to replace existing vegetation for scenario 2.

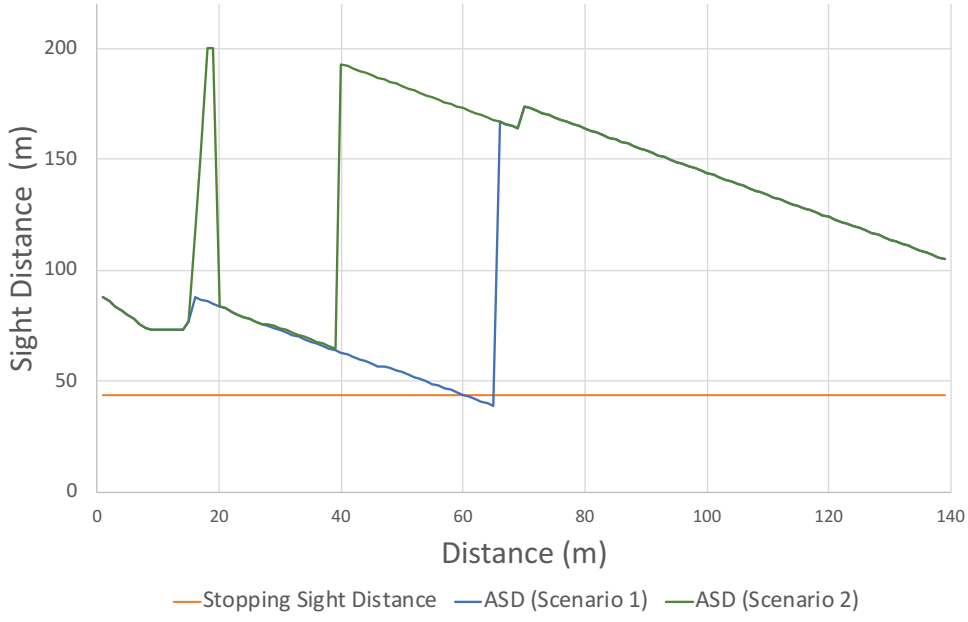

Figure 9. Comparison between required (orange) and available sight distances for scenarios 1 (in blue) and 2 (in green).

line displays the results obtained with the real vegetation, and the green line shows the results of scenario 2. These obstructions were located approximately 6 m apart from the intersection along Complutense Ave. (northbound direction), but they impacted several stations located behind them. A comparison of the two charts showed how the available sight distance varies in initial parts of the trajectory as the sightlines are not blocked by the branches that occupy the bikeway.

The replacement had effects in various stations along the trajectory. In scenario 1 stations 60 to 65 did not meet the required sight distance for stopping. They lacked up to 4 m to meet the required value. In scenario 2 all stations met the required stopping value. The evaluation of scenario 2 proved to be useful in determining what element caused the obstruction and quantifying the effects of its replacement/correction in terms of visibility.

3.2 Available vs intersection sight distances between riders

As the junction under study is signalized, conflicts between motorists and riders are accounted for by the traffic light. In that regard, some of the most common conflicts between riders along segregated bikeways and motorists are left- and right-hook collisions from turning traffic. In this intersection, these accidents could only happen if either of them disregards the traffic lights. After evaluating the allowed bikeway turns, two conflicts were found to not be

accounted for by the traffic lights. These two had to be evaluated as rolling and stopping, and the rest required the regular evaluation based on their intersection sight distances. The first unhandled trajectory is the right turn of cyclists riding northbound the main road (Complutense Ave.). These trajectories share conflict points with southbound riders, and both have the right to cross during the green phase. The second one is the left turn from the minor road (Novais St.) where conflict points are shared with Complutense Ave. users (both northbound and southbound). Results presented below correspond to the least favorable case, which is left turning users from Novais St. Intersection sight distances of rolling and stopped users were obtained with equation 2, using the posted speed limits of both streets. E-scooter riders and cyclists along the major road (30 km/h) required an intersection sight distance of 52.3 m; for the minor road the value was 44.11 m.

3.2.1 Available vs intersection sight distances: stopped users

The left-turning movement from Novais St. was found to be conflictive with both the northbound and southbound trajectories from Complutense Ave., which means that this evaluation would require two sight triangles, each starting at the decision point with their legs pointing to their respective conflictive user. Nonetheless, the stopped evaluation will consider the sight triangle whose area overlaps the roadway. Stations representing observers (stopped users) were located near and at the intersection's crossing with a separation of 1 m. Target stations were only evaluated with the eye-height of cyclists, due to the fact that bicyclists are the most common user present in riding facilities. In addition, target stations were located at distances equal to the intersection sight distance from the conflict point. This is based on the fact that target users are not considered to be coming to a full stop. This evaluation was performed considering two scenarios with different traffic volumes. The first one, scenario no. 3, was carried out considering the minor road (Novais St.) traffic-free. The second one, scenario no. 4, was carried out with the maximum flow that can be allowed. The files representing automobiles were as well obtained from Sketchup's warehouse (Trimble 2018) and the models chosen were those with more presence in the city's traffic mix (ANFAC 2018). These are displayed as gray elements in Figure 10, where aboveground elements are depicted in green and the DTM in shades of brown and gray.

Results from scenario 3 evidenced that cyclists located right at the crossing's edge were able to see 55.96 m ahead. This distance was the length of their longest unobstructed sightline, which is a larger value than their required sight distance (52.3 m). The same evaluation with the intersection at full capacity, scenario 4, revealed that these users are not able to see further the crossing, nor their trajectory or conflicting ones when located at distances up to 1 m apart from the crossing. Despite the fact that e-scooter riders have higher eye-height, their results were similar. Figure 11 shows the points where the interruptions of the cyclists' sightlines occurred, revealing the impacts of vegetation and present traffic. The red dots represent the positionings of the considered observers, and the green dots are the locations where their lines-of-sight were obstructed.

Figure 10. 3D model of the intersection with Novais Street busy. Automobiles are modeled as gray elements, aboveground elements in green and the DTM in shades of brown.

Figure 11. Intersection aerial photo showing observer and target positionings (red dots) and locations where the sightlines were blocked (green dots).

3.2.2 Available vs intersection sight distances: rolling users

Stations that represented the trajectories of rolling users covered a distance equal to the calculated intersection sight distance, measured from the conflict point. This was done along the trajectories of both observer and conflicting users as in this case, neither user is considered to be coming to a full stop. Target stations had the eye-height of other cyclists, as before. Figure 12 (a) shows the considered trajectories along the intersection with their required sight triangle (approach sight triangle). The red dots represent the observer positionings, and blue dots represent the stationing of conflictive users. Each user was positioned in the middle of their respective lane. Results showed that observers were capable of seeing 48% of their required sight triangle along their forthcoming trajectory (Figure 12 (b)). These percentages were obtained from the normalized percentage of the triangle covered by equally spaced (1 m), and unobstructed sightlines. These results showed that less than half of the required clear sight triangle were available to the observer, for that reason the intervisibility evaluation was carried out.

3.2.3 Intervisibility evaluation

A total of 12 thousand sightlines were obtained for both observers with codes from 0 to 1 depicting

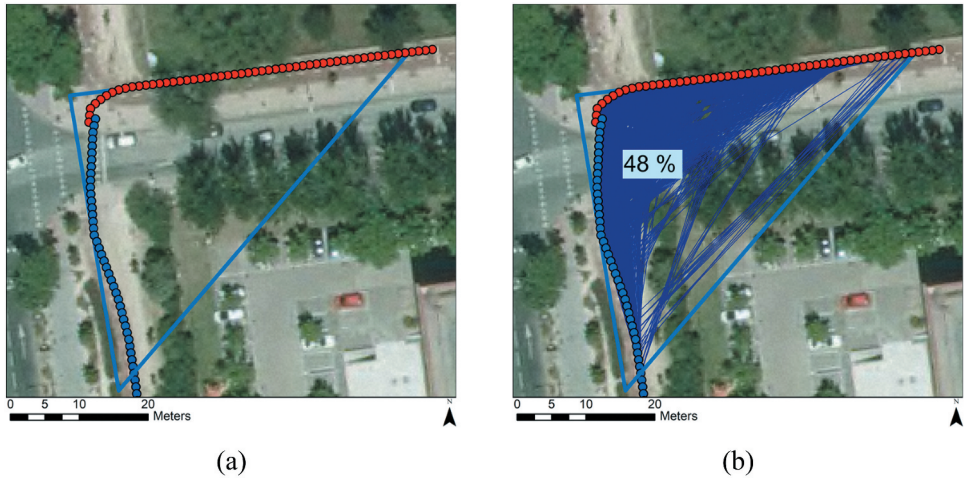

Figure 12. Left-turn evaluation with its required sight triangle (in light blue): (a) the red dots represent the observer positionings, and blue dots represent the stationing of conflictive users; (b) their unobstructed sightlines (in dark blue).

Table 1. Statistical results of the intervisibility analysis.

Level	Least Sq Mean	Mean[i]-Mean [j]	Std Error Diff
Observer 1 to observer 2	0.7631	0.1125	0.0078
Observer 2 to observer 1	0.6506		

whether they were able to see each other. Results of their statistical evaluation showed that the samples of sightlines were significantly different. The Least Significant Difference (LSD) was carried out for α = 5% and its value was 0.015. Table 1 summarizes the values obtained by analyzing the differences between samples.

The stations, along with the sight triangle and their unique identifiers, are presented in Figure 13. In terms of the overall intersection visibility, riders turning left are capable of seeing 35% of the required sight triangle for this movement. Those going northbound are able to see only 30% of the same triangle.

The following step is meant to evaluate the remaining conflicting trajectories of the intersection, specifically, the ones that are handled by the type of intersection control (traffic signal in this case) and could have new obstructions blocking their sight plane. Since the rest of the trajectories are handled by the traffic light, the AASHTO guidelines require a verification of the visibility from their approaches. The

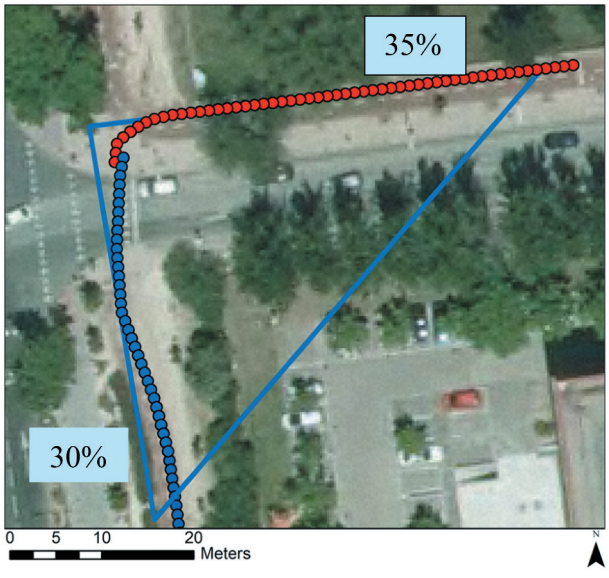

Figure 13. Summary of intervisibility analysis results. Visibility of riders turning left, 35%, northbound ones, 30%. Required sight triangle in light blue, riders positionings as dots.

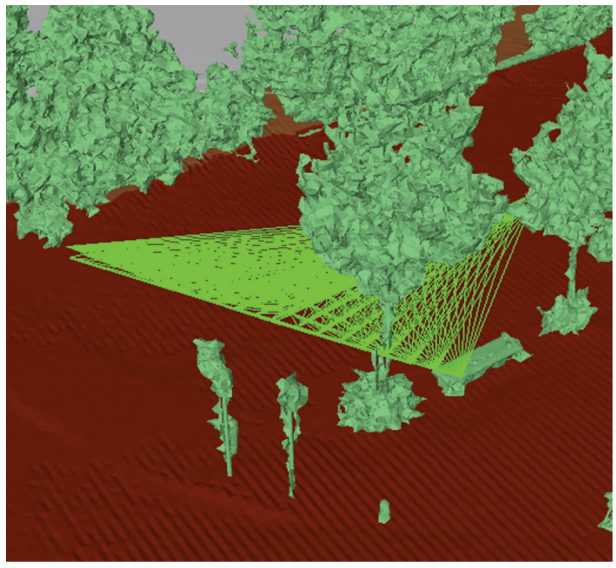

Figure 14. View of the clear zone (light green) required to avoid pedestrian-rider conflicts. Sightlines are represented by light green lines, aboveground elements are depicted in green and the DTM in shades of brown and gray.

evaluation carried out confirmed that the first road users of each approach are able to spot each other.

3.3 Conflicts between pedestrians and riders at sidepaths intersecting sidewalks

This verification was made on each side of the pedestrian crossing, before and after the crossing, modifying the evaluation established in the AASHTO guidelines by duplicating the triangles. All triangles were free of obstructions except the one that considered pedestrians along Novais St. versus bikeway users about to cross. Figure 14 shows the evaluation's obstructed sightlines. Green lines are the sightlines launched from the bikeway toward each side of the sidewalk. Despite the fact that 98% of the triangle is clear, few sightlines are blocked due to the presence of the tree.

4. Conclusions

As cycling and other sustainable transportation modes are varying in type, speed, and deployment, it is important to make sure present-day infrastructure and design cope with these changes delivering safe riding and walking facilities. In this regard, this paper aims to introduce a flexible procedure that could carry out visibility analyses considering a range of factors. This framework employs GIS functionalities to

evaluate road design elements with flexibility enough to cope with new transportation challenges, like accommodating these dissimilar users.

The selected case study helped to evidence the benefits that portable LiDAR systems offer to estimate visibility of segregated bikeways. Unfortunately, their relatively low productivity when compared to car-mounted or aerial LiDAR systems would prevent their use in large bicycle networks.

The presented procedure was tested by evaluating the required sight distance of a junction. This evaluation made sure that these facilities were consistent with design requirements. The stopping versus available sight distance analysis was positive as most of the trajectories had sufficient distances to carry out a stopping maneuver for all considered users except small areas blocked by vegetation. This effect was quantified by replacing real vegetation with 3D objects representing it.

Two considerations of riders (stopped and rolling) were introduced for those cases where conflictive trajectories are not accounted for by the type of control present at the intersection. These positions would allow the evaluation of sight distances when users are approaching the intersection and when stopped waiting for the right gap to cross. The evaluation of stopped users evidenced the impact of traffic volumes on their required sight distances. Rolling users, on the other hand, displayed unobstructed lines-of-sight that covered less than 50% of their required sight triangles. The intervisibility analysis showed which users of conflicting turns have clearer sights of opposing users. These results could be useful to aid decisions of which side of the bikeways could be improved. Finally, the pedestrian-rider evaluation gave insights into the conspicuousness between these two. Adequate sight lines so that bicyclists and pedestrians are able to see each other well in advance is an important safety aspect of sidepath-sidewalk intersections. This procedure helps to determine if road sections are in agreement with sight distance requirements set during their design. The presence of obstructions helps identify its nature, which could lead to basic maintenance works (vegetation or debris removal) or to be used in combination with other safety analyses in decision-making processes.

For future lines, the procedure is to be applied to more complex intersections and larger areas to assess its efficiency and improve its robustness. In addition, the impacts of gender, experience and ages are to be included in the estimation of both required and available sight distances.

Acknowledgements

The authors gratefully acknowledge the financial support of the *Ministerio de Economía y Competitividad* of Spain and the European Regional Development Fund (FEDER). Research Project TRA2015-63579-R (MINECO/FEDER).

Disclosure statement

No potential conflict of interest was reported by the author(s).

Funding

This work was supported by the Ministerio de Economía y Competitividad of Spain and the European Regional Development Fund (FEDER) [TRA2015-63579-R (MINECO/FEDER)].

ORCID

Keila González-Gómez http://orcid.org/0000-0001-6782-4678
Serafín López-Cuervo Medina http://orcid.org/0000-0003-2396-7815
María Castro http://orcid.org/0000-0001-8941-5795

Data availability statement:

Due to the nature of this research, participants of this study did not agree for their data to be shared publicly, so supporting data is not available.

References

AASHTO. 2012. *Guide for the Development of Bicycle Facilities, 4th Ed*. Washington, DC: AASHTO.

AASHTO. 2018. *A Policy on Geometric Design of Highways and Streets*. 8th ed. Washington, DC: AASHTO.

ANFAC, 2018. ANFAC [WWW Document]. "Matricul. Vehículos Tur. 2018." URL https://anfac.com/(accessed october 1 2020).

AUSTROADS. 2016. *Guide to Road Design Part 3: Geometric Design*. 3.3. ed. Sydney: Austroads.

AUSTROADS. 2017a. *Guide to Road Design Part 6A: Paths for Walking and Cycling*. 2nd ed. Sydney, Australia: Austroads. doi: 10.16309/j.cnki.1007-1776.2003.03.004.

AUSTROADS. 2017b. *Guide to Road Design. Part 4A: Unsignalised and Signalised Intersections*. 3rd ed. Sydney: Austroads.

Ayuntamiento de Madrid. 2008. "Criterios Para El Trazado Y Diseño De Las Vías Ciclistas." Madrid: Ayuntamiento de Madrid.

Bassani, M., N. Grasso, and M. Piras. 2015. "3D GIS Based Evaluation of the Available Sight Distance to Assess Safety of Urban Roads." *ISPRS - International Archives of the Photogrammetry, Remote Sensing and Spatial Information Sciences* XL-3/W3: 137–143. doi:10.5194/isprsarchives-XL-3-W3-137-2015.

Cai, Q., M. Abdel-Aty, and S. Castro. 2020. "Explore Effects of Bicycle Facilities and Exposure on Bicycle Safety at Intersections." *International Journal of Sustainable Transportation* 1–12. doi:10.1080/15568318.2020.1772415.

Cao, S., Q. Weng, M. Du, B. Li, R. Zhong, and Y. Mo. 2020. "Multi-scale Three-dimensional Detection of Urban Buildings Using Aerial LiDAR Data." *GIScience & Remote Sensing* 57 (8): 1125–1143. doi:10.1080/15481603.2020.1847453.

Castro, M., S. Lopez-Cuervo, M. Paréns-González, and C. De Santos-berbel. 2016. "LIDAR-based Roadway and Roadside Modelling for Sight Distance Studies." *Survey Review* 48 (350): 309–315. doi:10.1179/1752270615Y.0000000037.

Digi21, 2018. "Modelos Digitales Topográficos MDTopX [WWW Document]". Softw. MDTopX. URL https://www.digi21.net/MDTop (accessed 14 june 2018).

Gargoum, S. A., and K. El Basyouny. 2019. "A Literature Synthesis of LiDAR Applications in Transportation: Feature Extraction and Geometric Assessments of Highways." *GIScience & Remote Sensing* 56 (6): 864–893. doi:10.1080/15481603.2019.1581475.

González-Jorge, H., L. Díaz-Vilariño, H. Lorenzo, and P. Arias. 2016. "Evaluation of Driver Visibility from Mobile Lidar Data and Weather Conditions." *ISPRS - International Archives of the Photogrammetry, Remote Sensing and Spatial Information Sciences* XLI-B1: 577–582. 2016-Janua. doi:10.5194/isprsarchives-XLI-B1-577-2016.

Harwood, D. W., J. M. Mason, R. E. Brydia, M. T. Pietrucha, and G. L. Gittings, 1996. "National Cooperative Highway Research Program Report 383: Intersection Sight Distance." NCHRP. doi:10.1093/jicru/os20.1.report38.

Hassan, Y., S. M. Easa, and A. O. A. El Halim. 1996. "Analytical Model for Sight Distance Analysis on Three-dimensional Highway Alignments." *Transportation Research Record: Journal of the Transportation Research Board* 1523 (1): 1–10. doi:10.3141/1523-01.

Jung, J., M. J. Olsen, D. S. Hurwitz, A. G. Kashani, and K. Buker. 2018. "3D Virtual Intersection Sight Distance Analysis Using Lidar Data." *Transportation Research Part C: Emerging Technologies* 86: 563–579. doi:10.1016/j.trc.2017.12.004.

Karam, S., G. Vosselman, M. Peter, S. Hosseinyalamdary, and V. Lehtola. 2019. "Design, Calibration, and Evaluation of a Backpack Indoor Mobile Mapping System." *Remote Sensing* 11 (8): 905. doi:10.3390/rs11080905.

Khattak, A., S. Hallmark, and R. Souleyrette. 2003. "Application of Light Detection and Ranging Technology to Highway Safety." *Transportation Research Record: Journal of the Transportation Research Board* 1836 (1): 7–15. doi:10.3141/1836-02.

Khattak, A. J., and H. Shamayleh. 2005. "Highway Safety Assessment through Geographic Information System-Based Data Visualization." *Journal of Computing in Civil Engineering* 19 (4): 407–411. doi:10.1061/(ASCE)0887-3801(2005)19:4(407).

Leica Geosystems, 2020. "Leica Pegasus: BackpackWearable Mobile Mapping Solution | Leica Geosystems [WWW Document]." URL https://leica-geosystems.com/en-us/products/mobile-sensor-platforms/capture-platforms/leica-pegasus-backpack (accessed 20 august 2020).

López-Cuervo Medina, S., E. Pérez-Martín, T. R. H. Tejedor, J. F. Prieto, J. Velasco, M. Á. C. Martín, A. Ezquerra-Canalejo, and J. A. De Mata. 2019. "Assessment of DSMs Using Backpack-Mounted Systems and Drone Techniques to Characterise Ancient Underground Cellars in the Duero Basin (Spain)." *Sensors* (Switzerland). 19 (24): 5352. doi:10.3390/s19245352.

Ma, Y., Y. Zheng, J. Cheng, and Y. Zhang. 2019. "Hybrid Model for Realistic and Efficient Estimation of Highway Sight Distance Using Airborne LiDAR Data." *Journal of Computing in Civil Engineering* 33 (6): 04019039. doi:10.1061/(asce)cp.1943-5487.0000853.

Ministerio de Fomento. 2012. *Guía De Nudos Viarios*. Madrid: Ministerio de Fomento.

Ministerio de Fomento. 2016. *Norma 3.1-IC: Trazado, Boletín Oficial Del Estado*. Madrid: Ministerio de Fomento. doi:10.1017/CBO9781107415324.004.

National Highway Traffic Safety Administration. 2017. *Traffic Safety Facts 2015*. Washington, DC: U.S. Department of Transportation.

Olsen, M. J., D. Hurwitz, A. Kashani, and K. Buker. 2016. *3D Virtual Sight Distance Analysis Using Lidar Data*. Washington, DC: Pacific Northwest Transportation Consortium.

Romanillos, G., and J. Gutiérrez. 2019. "Cyclists Do Better. Analyzing Urban Cycling Operating Speeds and Accessibility." *International Journal of Sustainable Transportation* 14 (6): 448–464. doi:10.1080/15568318.2019.1575493.

Sanchez, E. 1995. "Three-Dimensional Analysis Of Sight Distance On Interchange Connectors." *Transportation Research Record* 1445: 101–108.

Stutts, J., and W. Hunter. 1999. *Injuries to Pedestrians and Bicyclists: An Analysis Based on Hospital Emergency Department Data*. Federal Highway Administration.

Trimble, 2018. "SketchUp [WWW Document]." URL https://www.sketchup.com/es/products/sketchup-free (accessed 11 july 2018).

Tsai, Y., Q. Yang, and Y. Wu. 2011. "Use of Light Detection and Ranging Data to Identify and Quantify Intersection Obstruction and Its Severity." *Transportation Research Record: Journal of the Transportation Research Board* 2241 (1): 99–108. doi:10.3141/2241-11.

Williams, L. J., and H. Abdi. 2010. *Encyclopedia of Research Design*. Thousand Oaks, CA: Sage.

Zhao, Y., B. Wu, J. Wu, S. Shu, H. Liang, M. Liu, V. Badenko, A. Fedotov, S. Yao, and B. Yu. 2020. "Mapping 3D Visibility in an Urban Street Environment from Mobile LiDAR Point Clouds." *GIScience & Remote Sensing* 57 (6): 797–812. doi:10.1080/15481603.2020.1804248.